

Synthesis of the GPR40 Partial Agonist MK-8666 through a Kinetically Controlled Dynamic Enzymatic Ketone Reduction

Alan M. Hyde,^{*,†} Zhijian Liu,^{*,†} Birgit Kosjek,[†] Lushi Tan,[†] Artis Klapars,[†] Eric R. Ashley,[†] Yong-Li Zhong,[†] Oscar Alvizo,[‡] Nicholas J. Agard,[‡] Guiquan Liu,[§] Xiuyan Gu,[§] Nobuyoshi Yasuda,[†] John Limanto,[†] Mark A. Huffman,[†] and David M. Tschaen[†]

[†]Process R&D Department, MRL, Merck & Co., Inc., Rahway, New Jersey 07065, United States

[‡]Codexis Inc., Redwood City, California 94063, United States

[§]Shanghai SynTheAll Pharmaceutical Co., Ltd., Jinshan District, Shanghai 201507, China

Supporting Information

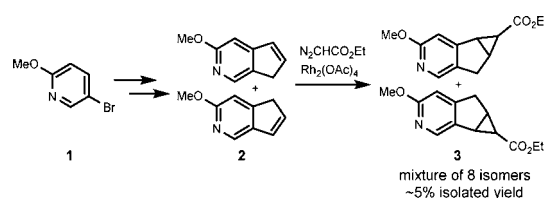


ABSTRACT: A scalable and efficient synthesis of the GPR40 agonist MK-8666 was developed from a simple pyridine building block. The key step to set the stereochemistry at two centers relied on an enzymatic dynamic kinetic reduction of an unactivated ketone. Directed evolution was leveraged to generate an optimized ketoreductase that provided the desired *trans* alcohol in >30:1 dr and >99% ee. Further, it was demonstrated that all four diastereomers of this hydroxy-ester could be prepared in high yield and selectivity. Subsequently, a challenging intramolecular displacement was carried out to form the cyclopropane ring system with perfect control of endo/exo selectivity. The endgame coupling strategy relied on a Pd-catalyzed C–O coupling to join the headpiece chloropyridine with the benzylic alcohol tailpiece.

Individuals afflicted with type II diabetes have long benefited from pharmaceutical intervention targeting insulin and/or glucose modulation. However, drug-induced hypoglycemia remains an ever-present risk to patients. The overarching theme of next-generation therapies is to provide feedback control that would prevent large disruptions to blood sugar homeostasis. A relatively new class of druggable targets being investigated to provide more stable glucose levels are free fatty acid receptors¹ (FFAs), with FFA1² (GPR40) garnering the most attention. In fact, a small molecule therapeutic was recently advanced to phase III clinical trials based on this mechanism.³ Given the aforementioned benefits of this modality coupled with our strong commitment to the diabetes field, MK-8666 was developed as a GPR40 partial agonist.⁴

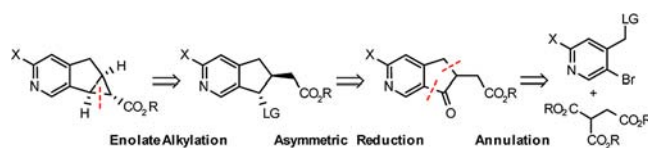
MK-8666 features an unusual pyridine-fused bicyclo[3.1.0]-hexane with three contiguous stereocenters. Retrosynthetically, the molecule can be roughly divided in half to give a biaryl portion referred to as the tailpiece and the tricyclic pyridine portion referred to as the headpiece (see abstract graphic). Synthesis of the tailpiece is described elsewhere⁵ and will not be the focus of this discussion. Scheme 1 depicts the early route to the headpiece^{4a} that commences with construction of indene 2 as a mixture of regioisomers from 5-bromo-2-methoxypyridine (1). The crux of this route was the cyclopropanation of 2 with ethyl diazoacetate that was poorly selective and gave 8 isomers. Although some aspects of this sequence were improved upon, it was deemed inadequate for further development and scale up.

Scheme 1. Discovery Route to the Tricyclic Headpiece



Given the difficulties encountered building the tricyclic ring system, subsequent efforts were spent on developing a practical and efficient approach for the production of clinical supply. We envisioned building the tricyclic ring system through an intramolecular enolate alkylation (Retrosynthesis in Scheme 2). This approach would require a *trans* alcohol or halide that ideally would be generated from a dynamic kinetic resolution.

Scheme 2. Retrosynthesis of the Tricyclic Headpiece



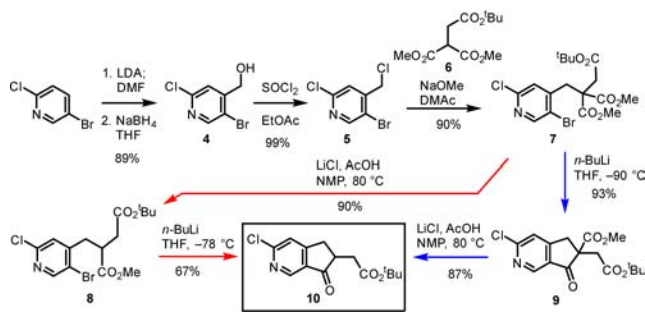
Received: October 3, 2016

Published: November 1, 2016

We anticipated building the ketone from a triester and a difunctionalized-5-halo-4-picoline.

To investigate this synthetic strategy, we first sought to establish an efficient synthesis of keto-ester **10** (Scheme 3). First,

Scheme 3. Synthesis of Ketone **10**



lithiation of 2-chloro-5-bromopyridine and quenching with DMF provided a 4-formylated pyridine that was used without isolation. Reduction with NaBH₄ gave alcohol **4**, which was then chlorinated with SOCl₂ to provide the chloromethylpyridine **5**. Alkylation of commercially available triester **6** with **5** was accomplished using NaOMe in DMAc to give **7**. The conversion of **7** to **10** was first demonstrated by decarboxylation with AcOH-buffered LiCl in NMP⁶ to generate diester **8** in 90% yield followed by lithiation/ring closure to provide ketone **10** in 67% yield. However, a higher yield of the lithiation/cyclization step was achieved when the sequence was reversed. We attribute this to triester **7** having one fewer enolizable center and being more electrophilic than diester **8**. In the event, lithium–bromide exchange and cyclization of compound **7** at –90 °C gave keto-diester **9** in 93% yield. Subsequent decarboxylation under similar reaction conditions proceeded smoothly to provide **10** in 87% yield.

At the outset, our strategy to access *trans* alcohol **11** rested on the premise that a dynamic asymmetric reduction of keto-ester **10** would set both adjacent stereocenters. We chose to focus on biocatalysis technology⁷ based on its proven reliability coupled with the diversity of commercially available ketoreductases (KREDs). Moreover, several enzymatic examples have been published, albeit mostly with α -keto esters and other activated systems having pK_a's ranging from 7 to 15.⁸ Even though ketone **10** was calculated to have a pK_a of 18.5 for the α -hydrogen (see Supporting Information (SI) pp S39–S40 for details), we were optimistic that epimerization through an enol pathway could take place at near-neutral pH.⁹

Initial screening of our KRED library under standard aqueous conditions at pH 7.0–8.0 revealed enzymes capable of providing three of the four possible diastereomers with high selectivity (Table 1). This, coupled with high conversions and rates, demonstrated the feasibility of the proposed dynamic kinetic reduction. Most enzymes favored the formation of the *cis* diastereomer (Table 1, entries 1–4). Similarly, the application of ruthenium-catalyzed transfer hydrogenation¹⁰ provided only the *cis* isomer **11b** in 94% ee (Table 1, entry 5). Unfortunately, only a small subset of enzymes were found that were selective in forming *trans* alcohols (Table 1, entries 6–8). The highest selectivity for the desired isomer **11** was obtained using KRED-208, achieving >99% ee, but a modest 2.4:1 *trans*/*cis* ratio (Table 1, entry 8).

With the aim to further improve selectivity, an investigation into the reaction kinetics of KRED-208 was undertaken. This

Table 1. Ketone Reduction Optimization, Enzyme Evolution

entry	catalyst	% conv	<i>trans</i> / <i>cis</i>	% 11a	% 11b	% 11c	% 11
1	KRED PIC1 ^a	95	<0.1:1	97	1	2	0
2	KRED PIH4 ^a	95	<0.1:1	95	0	0	5
3	KRED 131 ^a	100	0.2:1	0	82	18	0
4	KRED 136 ^a	100	<0.1:1	0	100	0	0
5	(<i>R,R</i>)-RuCl-TsDpen ^b	100	<0.1:1	3	97	0	0
6	KRED 124 ^a	95	7.3:1	0	12	88	0
7	KRED exp-BIT ^a	93	>50:1	1	1	94	4
8	KRED 208 ^a	97	2.4:1	30	0	0	70
9	KRED 264 ^c optimized enzyme	93	>30:1	2	0	0	98

^a2 g/L **10**, 100 wt % KRED, 1 g/L NADP, 0.1 M phosphate buffer pH 8.0, 30 °C. ^b0.075 M in ethyl acetate, 15 mol % catalyst, 5 equiv of formic acid, 2 equiv of DABCO. ^c50 g/L **10**, 2 wt % KRED, 0.1 g/L NADP, 0.1 M phosphate buffer pH 9.0, 50 °C, active nitrogen sweep.

revealed that the *cis* diastereomer **11a** was favored early (0.8:1 *trans*/*cis* at 17% conversion), but as the reaction proceeded, the *trans* isomer began forming preferentially, ultimately reaching a final ratio of ~2.4:1 *trans*/*cis* (Figure 1). Additional insight came

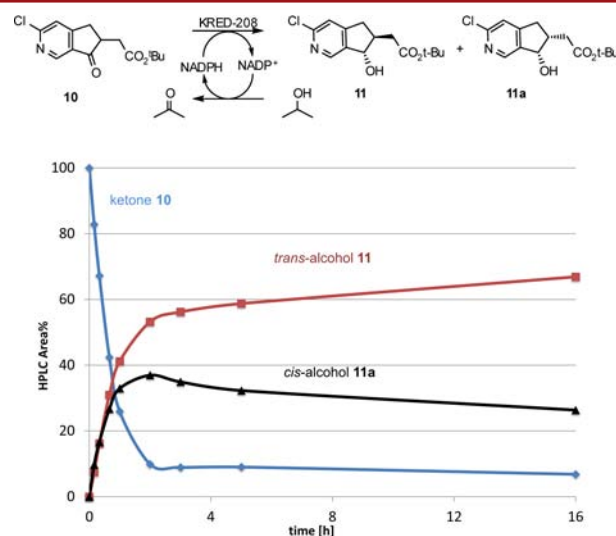


Figure 1. Kinetic profiling of KRED-208 activity.

from monitoring the ee of starting material which remained racemic throughout the reaction, indicating epimerization was fast with respect to ketone reduction.

A free energy diagram in Figure 2 illustrates how these observations can be rationalized. The initial slight intrinsic bias for the *cis* product can be traced to the difference in barrier heights on the red curve (ΔG_1^\ddagger). As the reaction proceeds, acetone builds up through 2-propanol oxidation and the equilibrium between alcohol products and ketone will become less favorable (reflected by ΔG_2) that results in a thermodynamically determined *cis*/*trans* ratio (ΔG_3). This is supported by calculations that predict the *trans* isomer to be between 0.4 and 1.4 kcal/mol more stable than the *cis* isomer (see SI p S37 for details). Entry to the blue curve is kinetically prevented, reflected

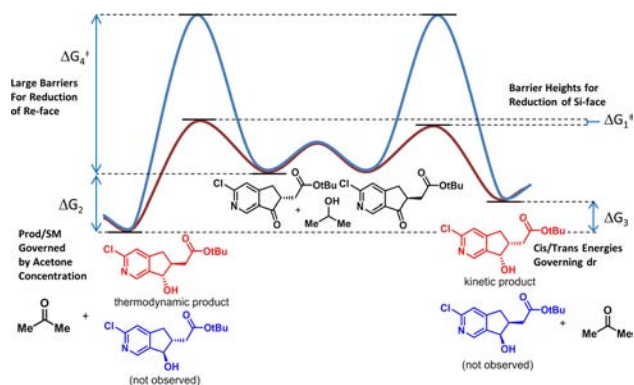


Figure 2. Free energy diagram of reduction with KRED-208.

by a large ΔG_4^\ddagger , because the enzyme active site is completely selective for hydride transfer to the Si-face of the ketone.

It became apparent that further progress toward developing a highly selective reaction would require two advances: (1) An enzyme with a significant intrinsic bias to generate the *trans* isomer and (2) preventing reversibility. The first would require an evolved enzyme¹¹ that provides improved diastereoselectivity. Reversibility could be addressed by removal of acetone with a nitrogen sweep.^{12,13} In partnership with Codexis Inc., six rounds of enzyme evolution delivered KRED-264, a novel variant able to produce **11** with >30:1 dr when a nitrogen sweep is utilized (Table 1, entry 9). This variant is also more active, requiring only 2 wt % loading with respect to ketone **10**. The optimized enzyme also exhibits high selectivity from the beginning and maintains it throughout the reaction course. With this development, we demonstrated the ability to access all four diastereomers¹⁴ of **11**.

Having a robust methodology in place for the preparation of **11**, we sought to affect the proposed cyclization (Table 2).¹⁶ The

Table 2. Optimization of Enolate Cyclization^a

entry	activating group	base	solvent	yield of 12
1	TsCl	Et ₃ N	THF	0 ^b
2	TsCl	LiHMDS	THF	5 ^b
3	(Me ₂ N) ₂ POCl	LiHMDS	THF	30 ^c
4	(PhO) ₂ POCl	LiHMDS	THF	60
5	(EtO) ₂ POCl	LiHMDS	THF	70
6	(EtO) ₂ POCl	LiHMDS	MTBE	94

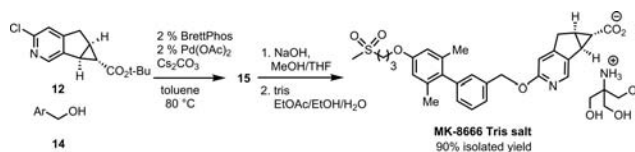
^aAll reactions were run for 16–24 h at –10 °C. ^bSignificant quantities of lactone **13** were generated. ^cDegradation of **12** was observed.

nature of the activating group had the greatest influence on the outcome of this transformation. For example, the sulfonate derived from TsCl in combination with a base primarily gave rise to lactone **13** (Table 2, entries 1, 2) arising from O-alkylation of the enolate with the strong leaving group. The use of a weaker leaving group such as a phosphate ester or phosphorodiamidate was critical to obtain the desired product (Table 2, entries 3–6).¹⁷ MTBE was a superior solvent for this transformation, and the desired cyclopropanation product was isolated in a 94% yield when (EtO)₂POCl was used in conjunction with LiHMDS

(Table 2, entry 6). Notably, the undesired *endo*-**12** product was never observed.¹⁸

With the headpiece in hand, installation of the tailpiece alcohol through S_NAr chemistry was nontrivial, failing with a wide variety of bases and solvents examined. In some cases, dimeric or ring-opened fragmentation products were identified. We attributed this outcome to the sensitive nature of the strained ring system with an acidic methylene position adjacent to the cyclopropane. Ultimately, it was found that chloropyridine **12** and alcohol **14** could be coupled to generate **15** in high yield (>90%) with a combination of Pd(OAc)₂, BrettPhos, and Cs₂CO₃ in toluene (Scheme 4).¹⁹ The rate of this reaction was sensitive to the

Scheme 4. C–O Coupling, Hydrolysis, and Salt Formation



source of Cs₂CO₃²⁰ which was problematic in light of the potential for decomposition. To address this, the base was milled to consistently achieve high reactivity. Cleavage of the *t*-Bu ester in **15** was accomplished with gentle heating in the presence of NaOH that avoided decomposition observed with acid-promoted conditions. Finally, the tris salt was isolated by crystallization from EtOAc/EtOH/water.

In summary, we have developed an efficient sequence to MK-8666 that utilized a novel enzymatic DKR reduction to set the absolute configuration and requisite *trans* configuration of a key intermediate. Mechanistic understanding of the kinetic and thermodynamic factors helped guide our development. The cyclopropane-forming step was only possible by carefully balancing the reactivity of the enolate/electrophile pair. The penultimate step made use of a Pd-catalyzed C–O coupling in which milling of the Cs₂CO₃ was deemed critical to obtain reproducible and robust results.

■ ASSOCIATED CONTENT

Supporting Information

The Supporting Information is available free of charge on the ACS Publications website at DOI: 10.1021/acs.orglett.6b02910.

Experimental procedures and characterization of new compounds, including their ¹H and ¹³C NMR spectra; details of DFT calculations with xyz coordinates and energies, for all stationary points (PDF)

■ AUTHOR INFORMATION

Corresponding Authors

*E-mail: alan_hyde@merck.com.

*E-mail: zhijian_liu@merck.com.

Notes

The authors declare no competing financial interest.

■ ACKNOWLEDGMENTS

We thank Jon Wilson, Steve Miller, and Kevin Belyk for catalyst screening; John Chung and Ed Sherer for calculating the energetics of *endo* vs *exo* ring closure; Bryon Simmons for contributing to finding conditions for the cyclopropane ring-closure; Jake Song for suggesting the use of phosphate ester

leaving groups; Shane Grosser and Zachary Dance for particle characterization of the Cs_2CO_3 ; Bob Reamer for providing NMR analytical assistance; and Wes Schafer and Becky Arvary for providing other analytical assistance (Merck & Co., Inc., Rahway, New Jersey, U.S.A.). We also thank Jin She, Yuhua Shi, Weifeng Hu, Yunchun Dai, Honglin Ye, and Xianliang He for additional experimental assistance (Shanghai SynTheAll Pharmaceutical Co., Ltd.).

REFERENCES

- (1) For a review on FFA targets, see: Ichimura, A.; Hasegawa, S.; Kasubuchi, M.; Kimura, I. *Front. Pharmacol.* **2014**, *5*, 1.
- (2) (a) Mancini, A. D.; Poitout, V. *Trends Endocrinol. Metab.* **2013**, *24*, 398. (b) Defossa, E.; Wagner, M. *Bioorg. Med. Chem. Lett.* **2014**, *24*, 2991.
- (3) (a) Srivastava, A.; Yano, J.; Hirozane, Y.; Kefala, G.; Gruswitz, F.; Snell, G.; Lane, W.; Ivetac, A.; Aertgeerts, K.; Nguyen, J.; Jennings, A.; Okada, K. *Nature* **2014**, *513*, 124. (b) Kaku, K.; Enya, K.; Nakaya, R.; Ohira, T.; Matsuno, R. *Diabetes, Obes. Metab.* **2015**, *17*, 675.
- (4) For the Med-Chem patent on GPR40 preclinical candidates including MK-8666, see: (a) Hagmann, W. K.; Nargund, R. P.; Blizzard, T. A.; Josien, H.; Biju, P.; Plummer, C. W.; Dang, Q.; Li, B.; Lin, L. S.; Cui, M., Antidiabetic tricyclic compounds. WO2014022528A1, February 6, 2014. For previous GPR40 preclinical candidates developed at Merck & Co., Inc., Kenilworth, NJ USA, see: (b) Tan, C. P.; Feng, Y.; Zhou, Y.-P.; Eiermann, G. J.; Petrov, A.; Zhou, C.; Lin, S.; Salituro, G.; Meinke, P.; Mosley, R.; Akiyama, T. E.; Einstein, M.; Kumar, S.; Berger, J. P.; Mills, S. G.; Thornberry, N. A.; Yang, L.; Howard, A. D. *Diabetes* **2008**, *57*, 2211. (c) Zhou, C.; Tang, C.; Chang, E.; Ge, M.; Lin, S.; Cline, E.; Tan, C. P.; Feng, Y.; Zhou, Y.-P.; Eiermann, G. J.; Petrov, A.; Salituro, G.; Meinke, P.; Mosley, R.; Akiyama, T. E.; Einstein, M.; Kumar, S.; Berger, J.; Howard, A. D.; Thornberry, N.; Mills, S. G.; Yang, L. *Bioorg. Med. Chem. Lett.* **2010**, *20*, 1298.
- (5) Goto, M.; Kajiura, T.; Kondo, Y.; Konishi, T.; Maeda, H.; Sera, M.; Yamano, M.; Yamasaki, S. Production Method of Optically Active Dihydrobenzofuran Derivatives U.S. Patent 8,952,185, August 23, 2012.
- (6) The use of AcOH was not required, but it was used to buffer chloride, thereby attenuating its reactivity to prevent unsafe exotherms.
- (7) For reviews on biocatalytic reductions, see: (a) Moore, J. C.; Pollard, D. J.; Kosjek, B.; Devine, P. N. *Acc. Chem. Res.* **2007**, *40*, 1412. (b) Gröger, H.; Hummel, W.; Metzner, R. In *Comprehensive Chirality*; Carreira, E. M.; Yamamoto, H., Eds.; 2012, *7*, 181–215. (c) Hall, M.; Bommaris, A. S. *Chem. Rev.* **2011**, *111*, 4088.
- (8) For a general review on enzymatic DKR reactions, see: (a) Applegate, G. A.; Berkowitz, D. B. *Adv. Synth. Catal.* **2015**, *357*, 1619. For examples of biocatalytic DKR reductions of diketones and ketoesters, see: (b) Kalaitzakis, D.; Smonou, I. *J. Org. Chem.* **2010**, *75*, 8658. (c) Kalaitzakis, D.; Rozzell, J. D.; Kambourakis, S.; Smonou, I. *Org. Lett.* **2005**, *7*, 4799. (d) Zhu, D.; Mukherjee, C.; Rozzell, J. D.; Kambourakis, S.; Hua, L. *Tetrahedron* **2006**, *62*, 901. (e) Kosjek, B.; Tellers, D. M.; Biba, M.; Farr, R.; Moore, J. C. *Tetrahedron: Asymmetry* **2006**, *17*, 2798.
- (9) A recent publication has described a DKR reduction of an unactivated ketone at near-neutral pH: Hanson, R. L.; Guo, Z.; González-Bobes, F.; Fenster, M. D. B.; Goswami, A. J. *Mol. Catal. B: Enzym.* **2016**, *133*, 20.
- (10) Akashi, M.; Arai, N.; Inoue, T.; Ohkuma, T. *Adv. Synth. Catal.* **2011**, *353*, 1955.
- (11) Bornscheuer, U. T.; Huisman, G. W.; Kazlauskas, R. J.; Lutz, S.; Moore, J. C.; Robins, K. *Nature* **2012**, *485*, 185.
- (12) Calvin, S. J.; Mangan, D.; Miskelly, I.; Moody, T. S.; Stevenson, P. *J. Org. Process Res. Dev.* **2012**, *16*, 82.
- (13) For a study on reversibility with various ketones, see: Tewari, Y. B.; Phinney, K. W.; Liebman, J. F. *J. Chem. Thermodyn.* **2006**, *38*, 388.
- (14) To the best of our knowledge, this is the first example of the feat. For an example with three out of four diastereomers using three different KREDs, see: (a) Lüdeke, S.; Richter, M.; Müller, M. *Adv. Synth. Catal.* **2009**, *351*, 253. For a two-step synthesis of four diastereomers, see: (b) Wolberg, M.; Hummel, W.; Müller, M. *Chem. - Eur. J.* **2001**, *7*, 4562.
- (15) For a review discussing enantioselective enzymes, see: Mugford, P. F.; Wagner, U. G.; Jiang, Y.; Faber, K.; Kazlauskas, R. J. *Angew. Chem., Int. Ed.* **2008**, *47*, 8782.
- (16) For a similar cyclization, see: Tan, L.; Yasuda, N.; Yoshikawa, N.; Hartner, F. W.; Eng, K. K.; Leonard, W. R.; Tsay, F.-R.; Volante, R. P.; Tillyer, R. D. *J. Org. Chem.* **2005**, *70*, 8027.
- (17) Song, Z. J.; Zhao, M.; Frey, L.; Li, J.; Tan, L.; Chen, C. Y.; Tschaen, D. M.; Tillyer, R.; Grabowski, E. J. J.; Volante, R.; Reider, P. J.; Kato, Y.; Okada, S.; Nemoto, T.; Sato, H.; Akao, A.; Mase, T. *Org. Lett.* **2001**, *3*, 3357.
- (18) This was rationalized with the aid of DFT calculations which shows a substantially higher kinetic barrier (4–5 kcal/mol) to form **endo-12** than **12**. See SI for transition state geometries and energies.
- (19) (a) Wu, X.; Fors, B.; Buchwald, S. L. *Angew. Chem., Int. Ed.* **2011**, *50*, 9943. (b) Kataoka, N.; Shelby, Q.; Stambuli, J. P.; Hartwig, J. F. *J. Org. Chem.* **2002**, *67*, 5553. (c) Maligres, P. E.; Li, J.; Krska, S. W.; Schreier, J. D.; Raheem, I. T. *Angew. Chem., Int. Ed.* **2012**, *51*, 9071.
- (20) For examples in which Cs_2CO_3 particle size is critical to cross-coupling reaction performance, see: (a) Betti, M.; Genesio, E.; Marconi, G.; Coccone, S. S.; Wiedenau, P. *Org. Process Res. Dev.* **2014**, *18*, 699. (b) Meyers, C.; Maes, B. U. W.; Loones, K. T. J.; Bal, G.; Lemièrre, G. L. F.; Dommissie, R. A. J. *Org. Chem.* **2004**, *69*, 6010.